JOURNAL OF THE ROYAL SOCIETY Interface

Plasma-sprayed $CaTiSiO_5$ ceramic coating on Ti-6Al-4V with excellent bonding strength, stability and cellular bioactivity

Chengtie Wu, Yogambha Ramaswamy, Xuanyong Liu, Guocheng Wang and Hala Zreiqat

J. R. Soc. Interface 2009 **6**, 159-168
doi: 10.1098/rsif.2008.0274

JOURNAL OF THE ROYAL SOCIETY Interface

J. R. Soc. Interface (2009) **6**, 159–168
doi:10.1098/rsif.2008.0274
Published online 29 July 2008

Plasma-sprayed $CaTiSiO_5$ ceramic coating on Ti-6Al-4V with excellent bonding strength, stability and cellular bioactivity

Chengtie Wu[1], Yogambha Ramaswamy[1], Xuanyong Liu[2], Guocheng Wang[2] and Hala Zreiqat[1,*]

[1]*Biomaterials and Tissue Engineering Research Unit, School of AMME, University of Sydney, Sydney 2006, Australia*
[2]*Shanghai Institute of Ceramics, Chinese Academy of Sciences, 1295 Dingxi Road, Shanghai 200050, People's Republic of China*

Novel Ca-Si-Ti-based sphene ($CaTiSiO_5$) ceramics possess excellent chemical stability and cytocompatibility. The aim of this study was to prepare sphene coating on titanium alloy (Ti-6Al-4V) for orthopaedic applications using the plasma spray method. The phase composition, surface and interface microstructure, coating thickness, surface roughness and bonding strength of the plasma-sprayed sphene coating were analysed using X-ray diffraction, scanning electron microscopy, atomic force microscopy and the standard mechanical testing of the American Society for Testing and Materials, respectively. The results indicated that sphene coating was obtained with a uniform and dense microstructure at the interface of the Ti-6Al-4V surface and the thickness and surface roughness of the coating were approximately 150 and 10 μm, respectively. Plasma-sprayed sphene coating on Ti-6Al-4V possessed a significantly improved bonding strength and chemical stability compared with plasma-sprayed hydroxyapatite (HAp) coating. Plasma-sprayed sphene coating supported human osteoblast-like cell (HOB) attachment and significantly enhanced HOB proliferation and differentiation compared with plasma-sprayed HAp coating and uncoated Ti-6Al-4V. Taken together, plasma-sprayed sphene coating on Ti-6Al-4V possessed excellent bonding strength, chemical stability and cellular bioactivity, indicating its potential application for orthopaedic implants.

Keywords: plasma spraying; surface modification; sphene; osteoblasts; titanium alloy

1. INTRODUCTION

The prevalence of primary and revision of total hip and knee arthroplasties increased steadily between 1990 and 2002 (Kurtz *et al.* 2005), and is expected to increase over the next two decades (Kurtz *et al.* 2007). Recently, the rate of joint replacement surgery has increased by 5–10 per cent per year, and over the past 20 years it has increased more than 10 per cent per year. Moreover, as many as 25 per cent of cementless hip replacements survive less than 10 years in young patients (Peter *et al.* 2005). Revision operations are mainly due to aseptic loosening of the implant following erosion of the supporting bone. Consequently, there is a need to develop new biocompatible surfaces that will anchor the implant device to the bone tissue in a strong and enduring manner.

A well-established primary biomaterial for orthopaedic implants is Ti-6Al-4V, a titanium alloy; however, it does not functionally integrate into bone. Various surface modification methods have been proposed for Ti-6Al-4V. The aim has been to enhance osseointegration and thereby interlock the implant with the surrounding skeletal tissue, which will provide a stable interface strong enough to support lifelong functional loading. Previous studies have shown that surface chemical modification of Ti-6Al-4V significantly enhanced the initial response, phenotype and signalling pathways of human osteoblasts (Zreiqat *et al.* 1999, 2002, 2005; Harle *et al.* 2006). Although these approaches have had some success, their major drawbacks are the slow rates of osseointegration and poor mechanical anchorage in challenging clinical cases (Sporer & Paprosky 2005).

Ti-6Al-4V coated with bioactive ceramics such as plasma-sprayed hydroxyapatite (HAp; Ha *et al.* 1998; Harle *et al.* 2006; Balani *et al.* 2007) and calcium silicate ($CaSiO_3$; Liu *et al.* 2001; Xue *et al.* 2005) showed improved stability of Ti-6Al-4V, providing a strong interface between the coating and the alloy and enhanced bone growth and mineralization (Soballe *et al.* 1991). However, these too have drawbacks (Kweh *et al.* 2002; Liu *et al.* 2004*a*,*b*; Xue *et al.* 2004). A crucial problem of Ti-6Al-4V-coated HAp is the poor bonding strength with the metal substrate due to the

*Author for correspondence (hzreiqat@usyd.edu.au).

Received 30 June 2008
Accepted 1 July 2008

mismatch of thermal expansion coefficient between HAp and Ti-6Al-4V (Liu *et al.* 2004*a*,*b*). The high residual stress resulting from the mismatch of the thermal expansion coefficient between HAp ($13.3\times10^{-6}\,K^{-1}$) and Ti-6Al-4V ($8.4\times10^{-6}$ to $8.8\times10^{-6}\,K^{-1}$) is thought to be responsible for the higher tensile stress and microcracks at the interface, which decreases the bonding strength between the two materials (HAp and Ti-6Al-4V) and limits their long-term survival (Kweh *et al.* 2002; Liu *et al.* 2004*a*,*b*; Xue *et al.* 2004).

Owing to their good bioactivity, $CaSiO_3$ ceramics have been used as coating on Ti-6Al-4V for biomedical applications (De Aza *et al.* 2000; Liu *et al.* 2004*a*,*b*; Xue *et al.* 2005). The results showed enhanced bonding strength of the plasma-sprayed $CaSiO_3$ coating, compared with HAp (e.g. Kweh *et al.* 2002; Liu *et al.* 2004*a*,*b*; Xue *et al.* 2005). However, like HAp, $CaSiO_3$ coatings have drawbacks, including their low chemical stability leading to degradation and instability of the coating after implantation (Liu *et al.* 2004*a*,*b*). Although $CaSiO_3$ coatings produced good bioactivity and enhanced short-term osseointegration properties of the implant (Xue *et al.* 2005), their poor chemical stability continues to be a major drawback and their long-term stability is questionable (Liu & Ding 2002; Wu *et al.* 2007*a*,*b*).

Sphene is a Ca-, Ti- and Si-containing mineral (Wu *et al.* 2007*a*,*b*) and, recently, we found that coating Ti-6Al-4V with sphene ceramic using the sol–gel method resulted in an improved adhesion strength and chemical stability of the coating compared with the sol–gel HAp coating (Wu *et al.* 2007*a*,*b*, 2008*a*–*c*, 2008). High temperature (more than 1000°C) is required to obtain a completely sintered and dense sphene, which is necessary to obtain good bonding strength of the coating. However, it cannot be applied when the sol–gel method is used to coat dense sphene on metals. Moreover, a temperature of more than 900°C will seriously oxidize and damage the Ti-6Al-4V surface. Plasma spraying, another common method often used to coat ceramics, avoids the above-mentioned drawbacks of the sol–gel method problem. Plasma spraying directly imposes extremely high temperatures on ceramic particles to melt/sinter them, but it avoids the direct exposure to high temperature of the Ti alloy substrate and hence avoids damaging the Ti alloy. The high temperature produced by the plasma spraying method is able to sinter and produce sphene coating with denser microstructure, compared with the sol–gel method. This will significantly improve the bonding strength of the coating on the Ti alloy (Liu *et al.* 2004*a*,*b*). In addition, the thermal expansion coefficient of sphene ($6\times10^{-6}\,K^{-1}$) is similar to that of Ti-6Al-4V (8.4×10^{-6} to $8.8\times10^{-6}\,K^{-1}$). Therefore, in the present study, we plasma sprayed sphene coating onto Ti-6Al-4V in an attempt to improve the bonding strength and compared their properties with sol–gel sphene coating and currently used plasma-sprayed HAp coating.

It is known that chemical composition (Zreiqat *et al.* 2005; Harle *et al.* 2006; Wei *et al.* 2008) and surface topography (Masaki *et al.* 2005; Liu *et al.* 2008) of the biomaterial can alter the cellular responses substantially. Recently, we showed that excellent human osteoblast-like cell (HOB) activity was obtained when the cells were cultured on dense sphene ceramic discs (Wu *et al.* 2007*a*,*b*). However, plasma-sprayed sphene coating has significantly different surface topography, roughness and microstructure compared with sphene ceramic discs, which could influence HOB activity. Therefore, in the present study, we aim to determine the effect of plasma-sprayed sphene coating on HOB attachment, proliferation and differentiation and compare their response with those cultured on HAp coating.

Table 1. Plasma spraying parameters.

argon plasma gas flow rate (slpm)	40
hydrogen plasma gas flow rate (slpm)	10
spray distance (mm)	100
argon powder carrier gas (slpm)	3.5
current (A)	600
voltage (V)	70

2. MATERIALS AND METHODS

2.1. Preparation of plasma-sprayed coating

Sphene powders were synthesized by the sol–gel process using tetraethyl orthosilicate ($(C_2H_5O)_4Si$, TEOS; Sigma Aldrich, USA), titanium (IV) butoxide ($Ti(O(CH_2)_3CH_3)_4$, $Ti(Bu)_4$; Sigma Aldrich, USA) and calcium nitrate tetrahydrate ($Ca(NO_3)_2\cdot4H_2O$; Sigma Aldrich, USA), as detailed previously (Wu *et al.* 2007*a*,*b*). Briefly, TEOS and $Ti(Bu)_4$ were mixed with ethanol and 2 M HNO_3 (molar ratio: TEOS/$Ti(Bu)_4$/ethanol/HNO_3 = 1 : 1 : 10 : 0.08) and hydrolysed for 30 min while stirring. $Ca(NO_3)_2\cdot4H_2O$ was added to the mixture (molar ratio: TEOS/$Ti(Bu)_4$/$Ca(NO_3)_2\cdot4H_2O$ = 1 : 1 : 1), and the reactants were stirred for 5 hours at room temperature followed by incubation at 60°C for 1 day before drying at 100°C for 2 days. The obtained dry gel was ground and transferred into a corundum crucible and calcined at 1100°C for 3 hours.

The calcined sphene powders were sieved to 80 mesh to get particles of 45–200 µm size, and then the sphene particles were sprayed onto Ti-6Al-4V discs (10×10×2 mm; Xi'an Continental Biomaterials Ltd Cor, China), using an atmosphere plasma spray system (APS-2000, Switzerland) and the parameters shown in table 1. Plasma-sprayed HAp coatings on Ti-6Al-4V substrates (HAp particle size: 45–160 µm) were prepared with same preparation conditions and used with uncoated Ti-6Al-4V as the controls. For cell culture, the Ti-6Al-4V discs were ultrasonically washed with water, acetone and ethanol for 10 min, respectively, and then dried at 40°C overnight.

2.2. Characterization of coating

The phase composition of the Ti-6Al-4V substrates before and after coating was analysed using X-ray diffraction (XRD; Siemens D5000, Germany) with a step size of 0.02° at a scanning rate of 1.2° min^{-1}. Surface morphology and roughness of the Ti-6Al-4V-coated discs were analysed using scanning electron

microscopy (SEM; Philips XL 30 CP, The Netherlands) and atomic force microscopy (AFM; Tempe, AZ, USA) in tapping mode. For evaluation of the coating thickness, inner microstructure and bonding interface, the coated discs were fixed in polymethylmethacrylate (PMMA) and sections were cut using a diamond saw (Exakt 300CL, Exakt Apparatebau, Germany) and subsequently ground and polished with an Exakt 400 CS Micro Grinding System (Exakt Apparatebau, Germany) before analysing by SEM. The open porosity of the coatings was tested by Archimedes' method.

2.3. Bonding strength and chemical stability of coating

For measuring the bonding strength, sphene coating with a thickness of approximately 380 μm was sprayed on Ti-6Al-4V rods with a diameter of 25 mm. The bonding strength between the coating and Ti-6Al-4V was measured in accordance with American Society for Testing and Materials C-633 (Liu *et al.* 2002; Xue *et al.* 2004).

For evaluation of the chemical stability of the coating, the coated discs were soaked in a buffer solution of tris(hydroxymethyl)aminomethane (Tris, $(CH_2OH)_3CNH_2$) and hydrochloric acid (HCl), with pH 7.4, for 1, 3 and 7 days, and the ratio of disc surface area and solution volume of Tris–HCl was 0.1 $cm^2\ ml^{-1}$. After soaking, the change of ion concentrations in Tris–HCl solution was analysed using inductively coupled plasma atomic emission spectroscopy (ICP-AES; Optima 3000 DV, PerkinElmer, USA) and the dissolution kinetic constant was calculated according to the released ion concentrations. The morphology of coating after soaking was analysed by SEM.

2.4. Isolation and culture of human osteoblast-like cells

HOB were grown from small pieces of vertebral bone harvested from healthy patients under 15 years of age undergoing orthopaedic procedures (Wu *et al.* 2007*a*,*b*, 2008*a*–*c*, 2008). Bone was morselized into approximately 1 mm^3 pieces, washed several times with phosphate-buffered saline (PBS) and digested for 90 min at 37°C with 0.02 per cent (w/v) trypsin (Sigma) in PBS. The digested cells were cultured in α-minimal essential medium (α-MEM; Gibco Laboratories), supplemented with 10 per cent (v/v) foetal calf serum (FCS; Gibco Laboratories), 2 mM L-glutamine (Gibco Laboratories, Grand Island, NY, USA), 25 mM Hepes buffer (Gibco Laboratories), 2 mM sodium pyruvate, 30 mg ml^{-1} penicillin, 100 mg ml^{-1} streptomycin (Gibco Laboratories) and 0.1 M L-ascorbic acid phosphate magnesium salt (Wako Pure Chemicals, Osaka, Japan). Then the digested cells were cultured in 75 cm^2 flasks at 37°C in a CO_2 incubator until confluence (approx. 70 per cent). The confluent cells were trypsinized and used for the attachment, proliferation and alkaline phosphatase assays. Permission to use discarded human tissue was granted by the Human Ethics Committee of the University of Sydney.

2.5. Attachment and morphology of HOB

HOB was cultured on sphene and HAp-coated Ti-6Al-4V discs placed in a 24-well culture plate at an initial density of 1×10^4 cells cm^{-2}. Cells were then incubated for 1, 3 and 7 days in α-MEM culture medium supplemented with 10 per cent FCS in humidified culture conditions. At the completion of culture, the discs were removed from the culture wells, rinsed with PBS (pH 7.4) and fixed with 1.25 per cent glutaraldehyde, 4 per cent paraformaldehyde and 4 per cent sucrose in PBS for 1 hour. The fixative was removed by washing with a buffer containing 4 per cent (w/v) sucrose in PBS and post-fixed in 1 per cent osmium tetroxide in PBS followed by sequential dehydration in graded ethanol (30, 50, 70, 90, 95, 100 per cent). Specimens were dried in hexamethyldisilizane for 3 min before coating with gold for SEM analysis. The morphological characteristics of attached cells on the coating discs were determined using SEM.

After 7 days of culture, the medium was collected from each well and ion concentrations were measured using ICP-AES.

2.6. Proliferation of HOB

The mitochondrial activity of the HOB cultured on coating and Ti-6Al-4V discs was determined by colorimetric assay, which detected the conversion of 3-(4,5-dimethylthiazol-2-yl)-2,5-diphenyltetrazolium bromide (MTS; Promega, Madison, WI, USA) to formazan, as detailed previously (Wu *et al.* 2008*a*–*c*, 2008). Cells were harvested with 0.1 per cent trypsin–EDTA solution in PBS and resuspended in full culture medium as detailed above. The cells were seeded at a concentration of 5×10^4 cells cm^{-2} onto the coating and the Ti-6Al-4V discs placed individually in a 24-well plate. Then the cells were left to grow for 1, 3 and 7 days at 37°C in a humidified atmosphere of 95 per cent air and 5 per cent CO_2. HAp-coated Ti-6Al-4V discs, uncoated Ti-6Al-4V discs and tissue culture plastic (TCP) templates were used as control. At days 1, 3 and 7, the discs were previously washed with 1× PBS. Freshly prepared MTS reaction mixture was diluted in PBS at a volume ratio of 1 : 5 (MTS : PBS) and added to the wells containing the discs and incubated at 37°C for 4 hours. Three specimens of each type were tested for each culture time point. One hundred microlitres of the converted 3-(4,5-dimethylthiazol-2-yl)-2,5-diphenyltetrazolium bromide from each well were transferred to a 96-well plate and the absorbance was recorded using a microplate reader (PathTech) at 490 nm using the software Accent.

2.7. Alkaline phosphatase (ALP) activity of HOB

The functionality of HOB cultured on the test and control discs was assessed by measuring the ALP activity using *p*-nitrophenyl phosphate substrate (ALP kit; Thermochem). The HOB were plated at a density of 5×10^4 cells cm^{-2} on the various discs and cultured for 1, 3 and 7 days. At the predetermined time point, the culture medium was decanted and the cell layer washed gently three times with 1× PBS followed by washing once with cold 50 mM Tris buffer, before lysing in Tris buffer containing 0.2 per cent NP-40

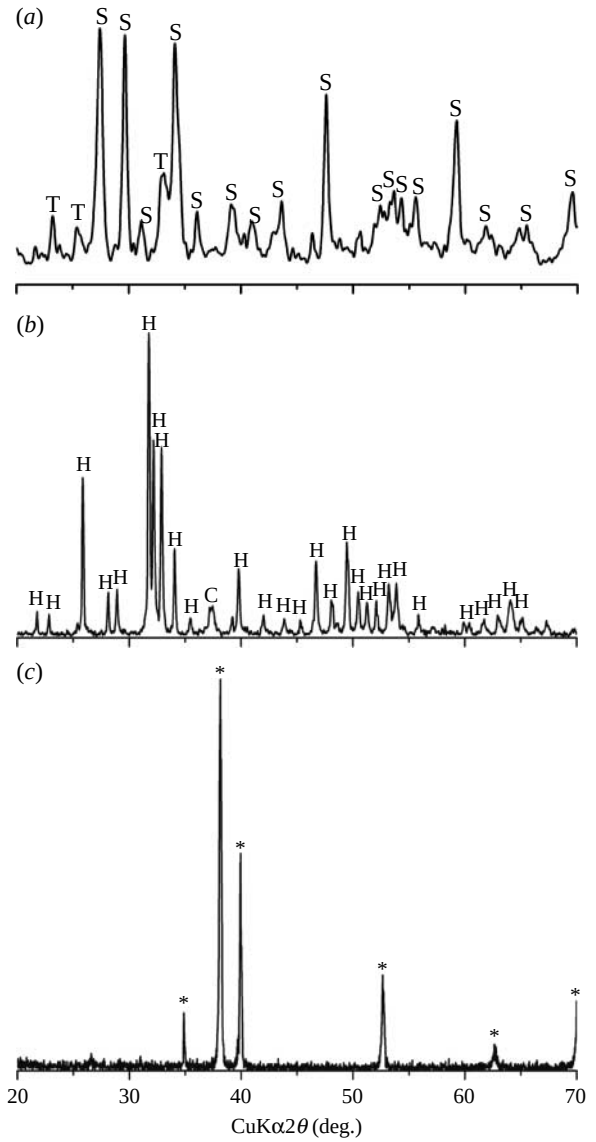

Figure 1. XRD analysis of (*a*) sphene and (*b*) hydroxyapatite coating and (*c*) Ti-6Al-4V substrates (asterisk denotes Ti-6Al-4V). S, sphene; T, $CaTiO_3$; H, HAp; C, CaO.

solution. The cells were sonicated for 20 s, centrifuged at 3000*g* for 5 min at 4°C and 2 µl of the lysate were added to 100 µl of 16.3 mmol l^{-1} *p*-nitrophenyl phosphate (Thermochem) in a 96-well plate and incubated for 30 min at 37°C. Reactions were stopped using 100 µl of 0.1 N NaOH and the absorbance read at 405 nm using a microplate reader (PathTech). The ALP activity was calculated from a standard curve after normalizing to the total protein content, which was measured using Pierce BCA protein assay kit, and the results expressed in millimolar *p*-nitrophenyl phosphate produced per minute per milligram of protein. ALP experiments were performed in triplicate and triplicate discs were used in each experiment.

2.8. Statistical analysis

The data were expressed as means ± standard deviation (s.d.) for all experiments and analysed using one-way ANOVA with *post hoc* test; $p<0.05$ was considered statistically significant.

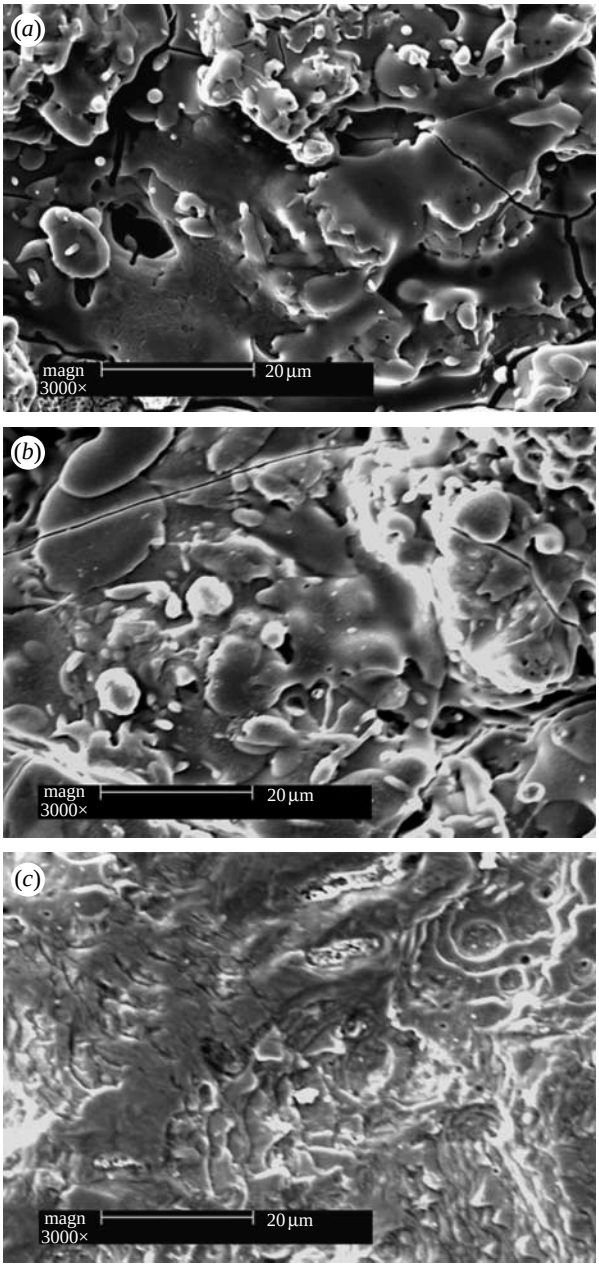

Figure 2. SEM morphology of (*a*) sphene and (*b*) hydroxyapatite coating and (*c*) Ti-6Al-4V discs.

3. RESULTS

3.1. Characterization of coating

XRD analysis shows that before coating, there are only characteristic peaks of Ti in the pattern (figure 1*c*), and after coating, sphene characteristic peaks (standard card no. JCPD 11-0142) and weak peaks of $CaTiO_3$ exist in the pattern of plasma-sprayed sphene coating (figure 1*a*). The plasma-sprayed HAp coating contains mainly HAp crystal phase (standard card no. JCPD 24-0033) and CaO phase in only minor amounts (figure 1*b*).

After plasma spray coating, the surface morphology of the Ti-6Al-4V discs changed significantly (figure 2). A compact sphene coating composed of melted sphene particles formed on the Ti-6Al-4V discs (figure 2*a*), with a morphology similar to that of the HAp coating (figure 2*b*). AFM analysis demonstrated that sphene-coated Ti-6Al-4V possesses a surface roughness similar

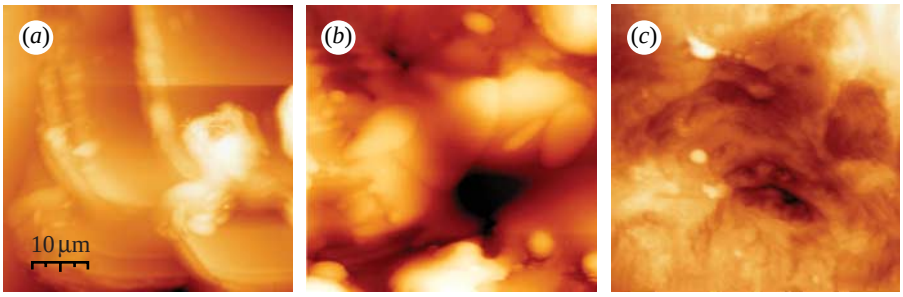

Figure 3. AFM analysis of the surface roughness: (*a*) sphene coating (R_a=10 µm), (*b*) HAp coating (R_a=10 µm) and (*c*) Ti-6Al-4V substrates (R_a=0.5 µm).

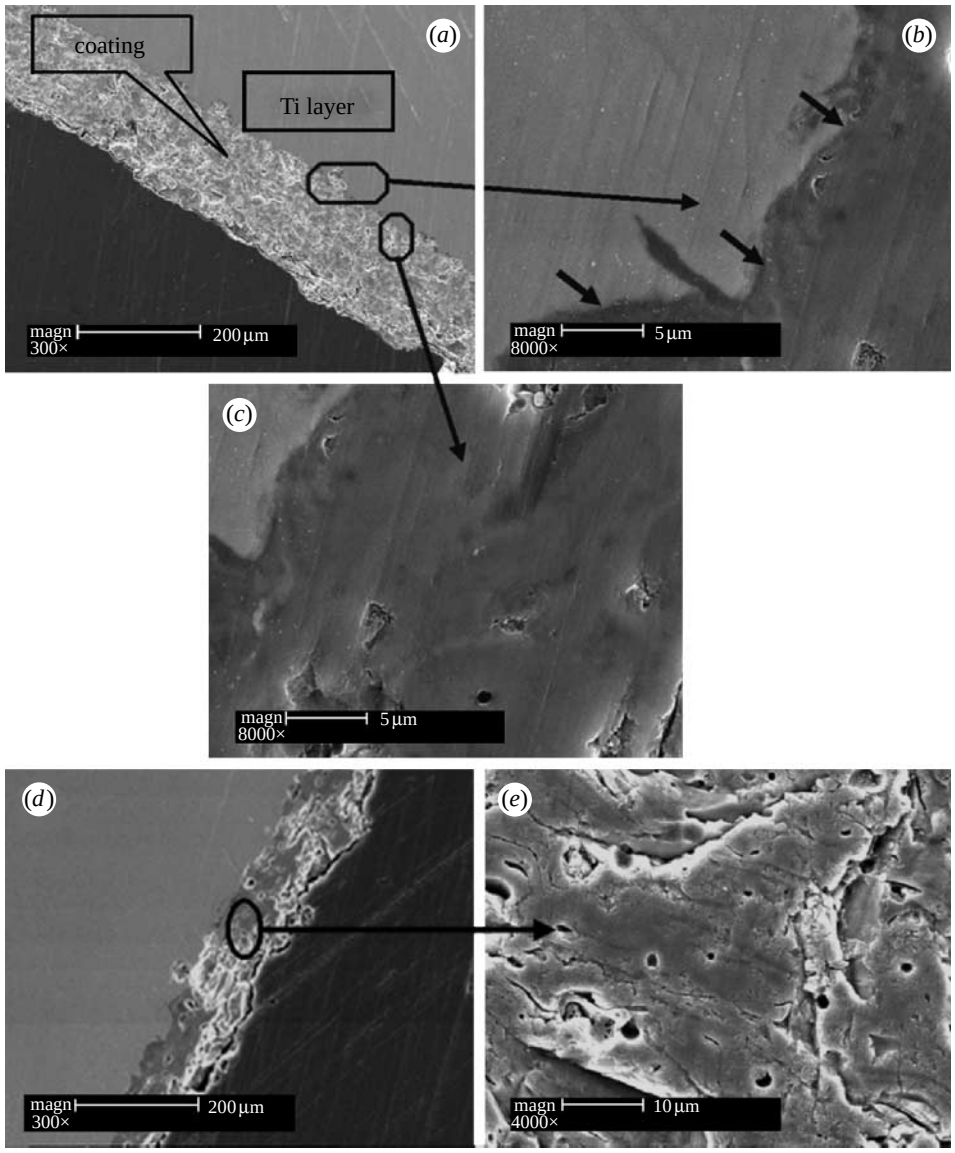

Figure 4. SEM cross section of sphene and HAp coating. (*a*) Thickness of sphene coatings is approximately 150 µm, (*b*) sphene coating and Ti-6Al-4V substrates forming a close interface as shown by arrows and (*c*) sphene coating possessing dense structure. (*d*) Cross section and (*e*) inner structure of HAp coatings.

to that of the HAp coating (10 µm), and both were significantly higher than that for the uncoated Ti-6Al-4V discs (0.50 µm; figure 3). The corresponding polished cross sections of the sphene and HAp coating are shown in figure 4. The thickness of the coating is approximately 150 µm (figure 4*a*). No microcracks were observed at the interface, indicating a close bonding between the coating and the Ti-6Al-4V substrates (figure 4*b*). The inner microstructure of sphene coating is highly dense and only a few micropores existed (figure 4*c*). The thickness of the HAp coating is approximately 140 µm (figure 4*d*) and a few micropores existed in the inner structure (figure 4*e*). The open porosity of the sphene and HAp coatings is 1.77±0.34 per cent and 3.04±0.66 per cent, respectively.

Table 2. Bonding strength of plasma-sprayed sphene and HAp coating.

coating	bonding strength (MPa)	references
plasma-sprayed sphene	33.2±2.4	
sol–gel sphene	17.4±0.9	Wu *et al.* (2008*a–c*, 2008)
plasma-sprayed HAp	5.9	Tsui *et al.* (1998)
	8.0–16.6	Khor *et al.* (1997, 1998)
	13.0	Zheng *et al.* (2000)
	24.5	Kweh *et al.* (2002)

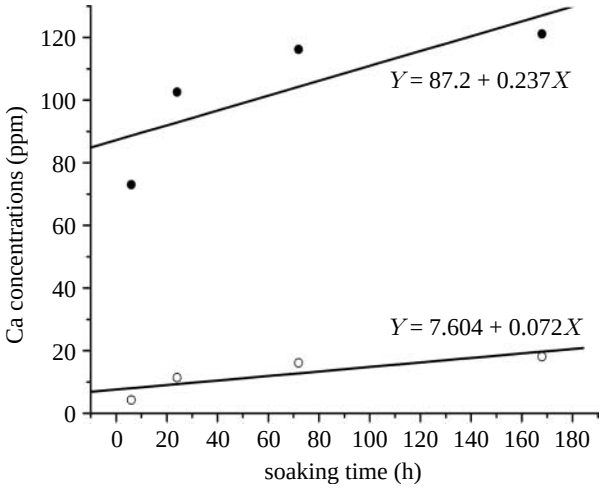

Figure 5. Ca dissolution kinetics of sphene (open circles) and HAp (filled circles) coating after 1, 3 and 7 days soaking in Tris–HCl solution by ICP-AES analysis.

3.2. Bonding strength and chemical stability of coating

The bonding strength of the plasma-sprayed sphene coating on Ti-6Al-4V was 33.2±2.4 MPa (table 2). ICP-AES analysis of Ca dissolution kinetics of the plasma-sprayed sphene and HAp coatings in Tris–HCl solutions is shown in figure 5. The concentration of the released Ca ions in Tris–HCl solution for sphene coating is significantly lower than that for HAp coating. Sphene coating has a lower dissolution kinetics constant (k=0.072 ppm h^{-1}) compared with that of HAp coating (k=0.237 ppm h^{-1}). SEM morphology analysis shows that after soaking in Tris–HCl for 7 days, sphene coating has no obvious change (figure 6*a*). However, the surface of HAp coating becomes coarse with some evidence of microparticles (figure 6*b*).

3.3. Attachment and morphology of HOB on coating

HOB attachment and morphology on sphene and HAp coating were examined using SEM. Sphene and HAp coatings supported HOB attachment after 1 and 3 days of culture (figure 7*a–d*) and cells were confluent and well spread on the two coatings after 7 days of culture (figure 7*e–h*).

3.4. Proliferation and ALP activity of HOB

At day 3, HOB proliferation on sphene coating is a little lower than that on HAp coating and comparable

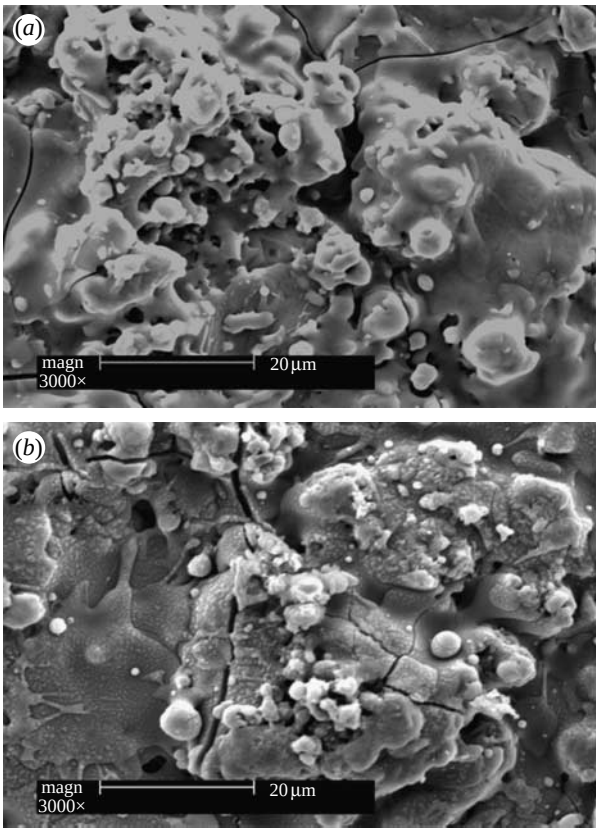

Figure 6. SEM morphology of (*a*) sphene and (*b*) hydroxyapatite coating after soaking in Tris–HCl for 7 days.

to Ti-6Al-4V and TCP (figure 8). However, by day 7, the HOB cultured on sphene-coated Ti-6Al-4V exhibited a significantly higher ($p<0.05$) proliferation than that on HAp coating, Ti-6Al-4V and TCP (figure 8). Figure 9 illustrates the changes in ALP activity of the HOB cultures at 1, 3 and 7 days. On days 1 and 3, the ALP activity is expressed at low levels for both sphene coating and controls. Thereafter, the ALP activity increased over time, and by day 7 was significantly higher ($p<0.05$) on sphene coating compared with HAp coating, Ti-6Al-4V and tissue culture plate (figure 9).

3.5. Ion concentration of culture medium

After 7 days of culture, the concentrations of Ca and Si ions in sphene coating-cultured medium are 2.85 and 0.29 mM, respectively, and no Ti ions are detected. There are no Si ions in HAp coating-cultured medium and TCP (table 3).

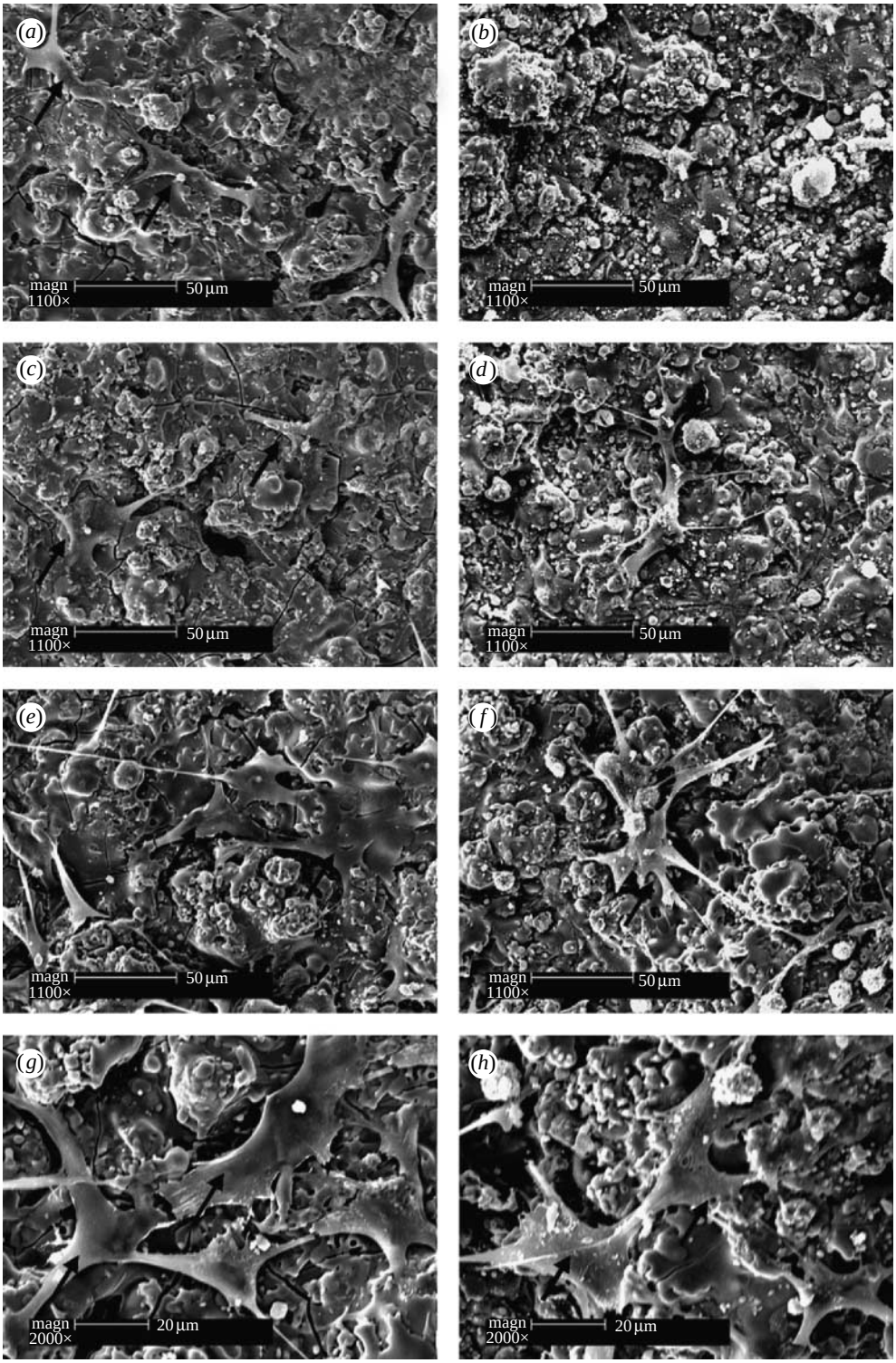

Figure 7. SEM of the attachment and morphology of human bone-derived cells cultured on sphene coating for (*a*) 1, (*c*) 3 and (*e*,*g*) 7 days, and on HAp coating for (*b*) 1, (*d*) 3 and (*f*,*h*) 7 days. (*g*) and (*h*) are higher magnification images. Arrows indicate cells.

4. DISCUSSION

The major finding of this study is that we developed for the first time the plasma-sprayed sphene-coated Ti-6Al-4V with significantly improved bonding strength, chemical stability and cellular bioactivity compared with the currently used HAp coating. HAp- and $CaSiO_3$-coated orthopaedic and dental implants have been widely studied for clinical trials and applications (Bauer *et al.* 1991; Kweh *et al.* 2002; Xue *et al.* 2005; Fini *et al.* 2008). However, the main drawbacks of these coatings are their poor bonding strength and insufficient chemical stability, which result in the delamination of coating from Ti alloys and limits their long-term survival (Khor *et al.* 1997; Kweh *et al.* 2002; Liu *et al.* 2004*a*,*b*; Xue *et al.* 2004). An important characteristic feature of a coated implant material is its sufficient bonding strength and chemical stability to maintain long-term functional loading. We showed that Ti-6Al-4V plasma-coated with

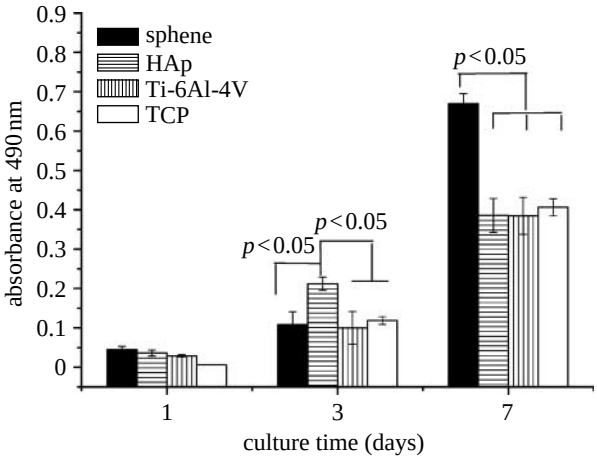

Figure 8. HOB proliferation on sphene, HAp coating and Ti-6Al-4V substrates at 1, 3 and 7 days of culture. TCP, tissue culture plate.

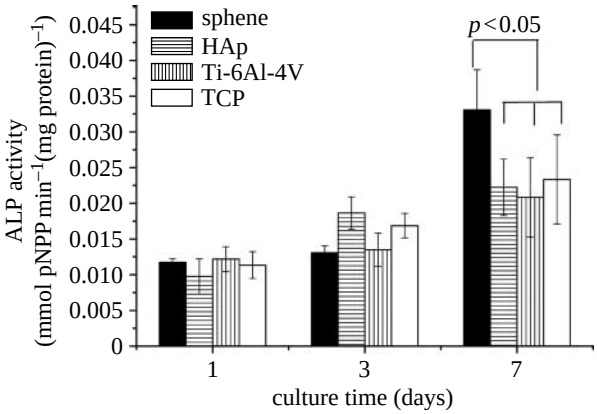

Figure 9. ALP activity of HOB on sphene, HAp coating and Ti-6Al-4V substrates at 1, 3 and 7 days of culture. TCP, tissue culture plate.

sphene possessed a significantly higher bonding strength (33.2 MPa), compared with HAp-coated Ti-6Al-4V (5.9–24.5 MPa; Khor *et al.* 1997, 1998; Tsui *et al.* 1998; Zheng *et al.* 2000; Kweh *et al.* 2002) and the sol–gel sphene coating (17.4 MPa; Wu *et al.* 2008*a–c*, 2008).

There are two important reasons for the excellent bonding strength of sphene plasma coating. One is the dense microstructure of sphene plasma coating. Previous studies have shown that the porosity of a coating has a significant effect on the bonding strength (Liu *et al.* 2004*a*,*b*; Oh *et al.* 2005). In this study, the porosity of sphene plasma coating (1.77 per cent) is lower than that of HAp plasma coating (3.04 per cent), which may contribute to the improved bonding strength of sphene plasma coating compared with HAp plasma coating. The sintering properties and powder shape may be the main factors affecting the coating density. Different ceramics have different sintering properties, such as sintering kinetics and shrinkage, at high temperature. Sphene may have better sintering properties that result in higher density. Although sphene and HAp powders have similar size distribution, however, the shape of powders may be a little different. Powder shape will affect powder flowability and further affect the coating density (Bartuli *et al.* 2002). In addition, the plasma spraying technique

Table 3. Ion concentrations of culture medium after 7 days of culturing HOB on coating and tissue culture plate (TCP).

coating	ion	concentration (mM)
sphene	Ca	2.85
	Si	0.29
	Ti	0
HAp	Ca	4.95
	Si	0
TCP	Ca	2.40
	Si	0

produced sphene coating with denser microstructure than the sol–gel technique. We recently demonstrated that sol–gel sphene coating possesses excellent chemical stability and enhanced bonding strength compared with sol–gel HAp-coated Ti-6Al-4V (Wu *et al.* 2008*a–c*, 2008). However, the sol–gel sphene coatings can only be sintered at relatively low temperature (less than 900°C) as higher temperature (more than 900°C) sintering will oxidize and damage the surface of the metal. The problem with low temperature (less than 900°C) sintering is that we cannot produce a completely dense structure of the sol–gel sphene coating, thus affecting its bonding strength. Plasma spraying is by far the most frequently used commercial technique for coating biomedical devices. The advantages of plasma spraying, compared with the sol–gel technique, include high deposition rates (80 g min^{-1}) and rough surface, which is favourable for bone substitutes (Liu *et al.* 2004*a*,*b*). The plasma spraying technique uses higher temperature compared with sol–gel coatings, producing dense microstructure and thereby denser bonding interface (Liu *et al.* 2004*a*,*b*).

Thermal expansion coefficient of ceramics (Saiz *et al.* 2002; Liu *et al.* 2004*a*,*b*) is another parameter that influences the bonding strength between the coatings and the underlying substrata. Sphene ceramics ($6\times10^{-6}\,K^{-1}$) possess a thermal expansion coefficient similar to that of Ti-6Al-4V (8.4×10^{-6} to $8.8\times10^{-6}\,K^{-1}$), therefore favouring a higher bonding strength and reducing the residual stress, which may result from the mismatch of the thermal expansion coefficient.

The chemical stability of the ceramics is an important factor influencing the long-term stability of the coating (Liu *et al.* 2004*a*,*b*; Wu *et al.* 2007*a*,*b*). In this study, we found that plasma-sprayed sphene coating has a decreased dissolution rate compared with HAp coating, indicating that sphene coating possesses an improved chemical stability, compared with HAp coating. Previous studies showed that the crystal structure of the ceramics affect their stability (Ducheyne *et al.* 1993; Radin & Ducheyne 1994). It is known that sphene and HAp ceramics have different crystal structures (sphene, monoclinic; HAp, hexagonal), which may result in the difference of the chemical stability of the two ceramic coatings.

The interaction of the cells with their substrate is a key factor for cellular activity including attachment, proliferation and differentiation (Anselme 2000), ultimately determining the cellular phenotype on the

biomaterials. The results of the present study indicate that plasma-sprayed sphene-coated Ti-6Al-4V supported HOB attachment and spreading, and significantly enhanced HOB proliferation and ALP activity compared with plasma-sprayed HAp coating and uncoated Ti-6Al-4V substrates, indicating an excellent cellular bioactivity. Zreiqat *et al.* have shown that chemical composition (Zreiqat *et al.* 2002, 2005; Wei *et al.* 2008) and surface topography (Liu *et al.* 2008) of the biomaterial can alter the cellular responses substantially. The chemical composition of the plasma-sprayed sphene coating is significantly different from that of the HAp coating and the Ti-6Al-4V substrates. Moreover, we found that sphene and HAp-coated Ti-6Al-4V have similar surface topography and roughness, but differ significantly in their chemical composition. Sphene is a Ca-, Ti- and Si-containing ceramic, while HAp is a Ca- and P-containing ceramic. Therefore, it is plausible to speculate that the different chemical composition between the two ceramics (sphene versus HAp) is the major contributor to the differences seen in the cellular responses to both coatings.

Previous studies have shown that ionic environment, caused by the dissolution of ions from biomaterials, has an important impact on the biological responses of cells (Valerio *et al.* 2004; Wu *et al.* 2005). Differences in materials' chemical composition will result in different ionic environments (Wu *et al.* 2006, 2007*a*,*b*) presented to the cells. Ions such as Ca and Si play a significant role in stimulating osteoblast proliferation, differentiation and regulation of their gene expression (Silver *et al.* 2001; Wu & Chang 2007; Wu *et al.* 2007*a*,*b*). In the present study, minor amounts of Ca and Si ions were released from the sphene coating (table 3), which may have contributed to the improved cellular activity. In addition, we found no detectable levels of Ti ions in the culture medium (Ti ion concentration was lower than the testing limit of ICP-AES (0.00X ppm)). Normal concentration of Ti in human tissue is 0.2 ppm (Hildebrand & Hornez 1998), and around the titanium implants no clinical tissue toxicity has been observed at local Ti concentrations of higher than 2000 ppm (Hildebrand & Hornez 1998). Therefore, the trace amount of Ti ions released from the sphene coating is very unlikely to result in toxic effects on human tissue.

5. CONCLUSIONS

Plasma-sprayed sphene coating on Ti-6Al-4V has been successfully prepared and demonstrates a close bonding with the Ti-6Al-4V substrate. The coating possesses a significantly improved bonding strength and chemical stability and enhanced HOB proliferation and differentiation, compared with plasma-sprayed HAp coating and uncoated Ti-6Al-4V. Taken together, plasma-sprayed sphene coating on Ti-6Al-4V possessed excellent bonding strength, chemical stability and cellular bioactivity, indicating its potential application as a coating for orthopaedic implants.

The authors would like to acknowledge the Australian National Health and Medical Research Council, the Australian Research Council, the National Basic Research Fund of China (grant no. 2005CB623901), Shanghai Science and Technology R&D Fund (grant no. 07QH14016) and the University of Sydney Research Fellowship (Dr Wu) for funding this research, Dr Wenrong Yang for his help in the AFM test and Assistant Professor Colin Dunstan for proofreading the manuscript.

REFERENCES

Anselme, K. 2000 Osteoblast adhesion on biomaterials. *Biomaterials* **21**, 667–681. (doi:10.1016/S0142-9612(99)00242-2)

Balani, K., Chen, Y., Harimkar, S. P., Dahotre, N. B. & Agarwal, A. 2007 Tribological behavior of plasma-sprayed carbon nanotube-reinforced hydroxyapatite coating in physiological solution. *Acta Biomater.* **3**, 944–951. (doi:10.1016/j.actbio.2007.06.001)

Bartuli, C., Valente, T. & Tului, M. 2002 Plasma spray deposition and high temperature characterization of ZrB2–SiC protective coatings. *Surf. Coat. Technol.* **155**, 260–273. (doi:10.1016/S0257-8972(02)00058-0)

Bauer, T. W., Geesink, R. C., Zimmerman, R. & McMahon, J. T. 1991 Hydroxyapatite-coated femoral stems. Histological analysis of components retrieved at autopsy. *J. Bone Joint Surg. Am.* **73**, 1439–1452.

De Aza, P. N., Luklinska, Z. B., Martinez, A., Anseau, M. R., Guitian, F. & De Aza, S. 2000 Morphological and structural study of pseudowollastonite implants in bone. *J. Microscopy* **197**, 60–67. (doi:10.1046/j.1365-2818.2000.00647.x)

Ducheyne, P., Radin, S. & King, L. 1993 The effect of calcium phosphate ceramic composition and structure on *in vitro* behavior. I. Dissolution. *J. Biomed. Mater. Res.* **27**, 25–34. (doi:10.1002/jbm.820270105)

Fini, A. M., Bracci, B., Boanini, E., Torricelli, P., Giavaresi, G., Aldini, N., Facchini, A., Sbaiz, F. & Giardino, R. 2008 The response of bone to nanocrystalline hydroxyapatite-coated Ti13Nb11Zr alloy in an animal model. *Biomaterials* **29**, 1730–1736. (doi:10.1016/j.biomaterials.2007.12.011)

Ha, S. W., Reber, R., Eckert, K. L., Petitmermet, M., Mayer, J., Wintermantel, E., Baerlocher, C. & Gruner, H. 1998 Chemical and morphological changes of vacuum–plasma-sprayed hydroxyapatite coatings during immersion in simulated physiological solutions. *J. Am. Ceram. Soc.* **81**, 81–88.

Harle, J., Kim, H. W., Mordan, N., Knowles, J. C. & Salih, V. 2006 Initial responses of human osteoblasts to sol–gel modified titanium with hydroxyapatite and titania composition. *Acta Biomater.* **2**, 547–556. (doi:10.1016/j.actbio.2006.05.005)

Hildebrand, H. & Hornez, J. 1998 Biological response and biocompability. In *Metals as biomaterials* (eds J. A. Helsen & H. J. Breme), pp. 265–290. Chichester, UK: Wiley.

Khor, K., Yip, C. & Cheang, P. 1997 Ti- 6Al-4V/hydroxyapatite composite coatings prepared by thermal spray techniques. *J. Therm. Spray Technol.* **6**, 109–115. (doi:10.1007/BF02646320)

Khor, K., Cheang, P. & Wang, Y. 1998 Plasma spraying of combustion flame spheroidized hydroxyapatite (HA) powders. *J. Therm. Spray Technol.* **7**, 254–260. (doi:10.1361/105996398770351007)

Kurtz, S., Mowat, F., Ong, K., Chan, N., Lau, E. & Halpern, M. 2005 Prevalence of primary and revision total hip and knee arthroplasty in the United States from 1990 through 2002. *J. Bone Joint Surg. Am.* **87**, 1487–1497. (doi:10.2106/JBJS.D.02441)

Kurtz, S., Ong, K., Lau, E., Mowat, F. & Halpern, M. 2007 Projections of primary and revision hip and knee arthroplasty in the United States from 2005 to 2030. *J. Bone Joint Surg. Am.* **89**, 780–785. (doi:10.2106/JBJS.F.00222)

Kweh, S. W., Khor, K. A. & Cheang, P. 2002 An *in vitro* investigation of plasma sprayed hydroxyapatite (HA) coatings produced with flame-spheroidized feedstock. *Biomaterials* **23**, 775–785. (doi:10.1016/S0142-9612(01)00183-1)

Liu, X. & Ding, C. 2002 Plasma sprayed wollastonite/TiO_2 composite coatings on titanium alloys. *Biomaterials* **23**, 4065–4077. (doi:10.1016/S0142-9612(02)00143-6)

Liu, X., Ding, C. & Wang, Z. 2001 Apatite formed on the surface of plasma-sprayed wollastonite coating immersed in simulated body fluid. *Biomaterials* **22**, 2007–2012. (doi:10.1016/S0142-9612(00)00386-0)

Liu, X., Tao, S. & Ding, C. 2002 Bioactivity of plasma sprayed dicalcium silicate coatings. *Biomaterials* **23**, 963–968. (doi:10.1016/S0142-9612(01)00210-1)

Liu, X. Y., Chu, P. K. & Ding, C. X. 2004*a* Surface modification of titanium, titanium alloys, and related materials for biomedical application. *Mater. Sci. Eng. R* **47**, 49–121. (doi:10.1016/j.mser.2004.11.001)

Liu, X., Ding, C. & Chu, P. K. 2004*b* Mechanism of apatite formation on wollastonite coatings in simulated body fluids. *Biomaterials* **25**, 1755–1761. (doi:10.1016/j.biomaterials.2003.08.024)

Liu, X., Lim, J., Donahue, H., Dhurjati, R., Mastro, A. & Vogler, E. 2008 Influence of substratum surface chemistry/energy and topography on the human fetal osteoblastic cell line hFOB 1.19: phenotypic and genotypic responses observed *in vitro*. *Biomaterials* **28**, 4535–4550. (doi:10.1016/j.biomaterials.2007.06.016)

Masaki, C., Schneider, G. B., Zaharias, R., Seabold, D. & Stanford, C. 2005 Effects of implant surface microtopography on osteoblast gene expression. *Clin. Oral Implants Res.* **16**, 650–656. (doi:10.1111/j.1600-0501.2005.01170.x)

Oh, I. H., Nomura, N., Chiba, A., Murayama, Y., Masahashi, N., Lee, B. T. & Hanada, S. 2005 Microstructures and bond strengths of plasma-sprayed hydroxyapatite coatings on porous titanium substrates. *J. Mater. Sci. Mater. Med.* **16**, 635–640. (doi:10.1007/s10856-005-2534-4)

Peter, B. *et al.* 2005 Calcium phosphate drug delivery system: influence of local zoledronate release on bone implant osteointegration. *Bone* **36**, 52–60. (doi:10.1016/j.bone.2004.10.004)

Radin, S. R. & Ducheyne, P. 1994 Effect of bioactive ceramic composition and structure on *in vitro* behavior. III. Porous versus dense ceramics. *J. Biomed. Mater. Res.* **28**, 1303–1309. (doi:10.1002/jbm.820281108)

Saiz, E., Goldman, M., Gomez-Vega, J., Tomsia, A., Marshall, G. & Marshall, S. 2002 *In vitro* behavior of silicate glass coatings on Ti6Al4V. *Biomaterials* **23**, 3749–3756. (doi:10.1016/S0142-9612(02)00109-6)

Silver, I. A., Deas, J. & Erecinska, M. 2001 Interactions of bioactive glasses with osteoblasts *in vitro*: effects of 45S5 bioglass, and 58S and 77S bioactive glasses on metabolism, intracellular ion concentrations and cell viability. *Biomaterials* **22**, 175–185. (doi:10.1016/S0142-9612(00)00173-3)

Soballe, K., Hansen, E. S., Brockstedt-Rasmussen, H., Hjortdal, V. E., Juhl, G. I., Pedersen, C. M., Hvid, I. & Bunger, C. 1991 Gap healing enhanced by hydroxyapatite coating in dogs. *Clin. Orthop. Relat. Res.* 300–307. (doi:10.1097/00003086-199111000-00045)

Sporer, S. M. & Paprosky, W. G. 2005 Biologic fixation and bone ingrowth. *Orthop. Clin. North Am.* **36**, 105–111. (doi:10.1016/j.ocl.2004.06.007)

Tsui, Y. C., Doyle, C. & Clyne, T. W. 1998 Plasma sprayed hydroxyapatite coatings on titanium substrates. Part 2: optimisation of coating properties. *Biomaterials* **19**, 2031–2043. (doi:10.1016/S0142-9612(98)00104-5)

Valerio, P., Pereira, M. M., Goes, A. M. & Leite, M. F. 2004 The effect of ionic products from bioactive glass dissolution on osteoblast proliferation and collagen production. *Biomaterials* **25**, 2941–2948. (doi:10.1016/j.biomaterials.2003.09.086)

Wei, J., Heo, S. J., Kim, D. H., Kim, S. E., Hyun, Y. T. & Shin, J. W. 2008 Comparison of physical, chemical and cellular responses to nano- and micro-sized calcium silicate/poly(ε-caprolactone) bioactive composites. *J. R. Soc. Interface* **5**, 617–630. (doi:10.1098/rsif.2007.1267)

Wu, C. & Chang, J. 2007 Synthesis and *in vitro* bioactivity of bredigite powders. *J. Biomater. Appl.* **21**, 251–263. (doi:10.1177/0885328206062360)

Wu, C., Chang, J., Wang, J., Ni, S. & Zhai, W. 2005 Preparation and characteristics of a calcium magnesium silicate (bredigite) bioactive ceramic. *Biomaterials* **26**, 2925–2931. (doi:10.1016/j.biomaterials.2004.09.019)

Wu, C., Chang, J., Ni, S. & Wang, J. 2006 *In vitro* bioactivity of akermanite ceramics. *J. Biomed. Mater. Res. A* **76**, 73–80.

Wu, C., Chang, J., Zhai, W. & Ni, S. 2007*a* A novel bioactive porous bredigite ($Ca_7MgSi_4O_{16}$) scaffold with biomimetic apatite layer for bone tissue engineering. *J. Mater. Sci. Mater. Med.* **18**, 857–864. (doi:10.1007/s10856-006-0083-0)

Wu, C., Ramaswamy, Y., Kwik, D. & Zreiqat, H. 2007*b* The effect of strontium incorporation into $CaSiO_3$ ceramics on their physical and biological properties. *Biomaterials* **28**, 3171–3181. (doi:10.1016/j.biomaterials.2007.04.002)

Wu, C., Ramaswamy, Y., Soeparto, A. & Zreiqat, H. 2008*a* Incorporation of titanium into calcium silicate improved their chemical stability and biological properties. *J. Biomed. Mater. Res. A* **86**, 402–410. (doi:10.1002/jbm.a.31623)

Wu, C., Ramaswamy, Y., Boughton, P. & Zreiqat, H. 2008*b* Improvement of mechanical and biological properties of porous CaSiO(3) scaffolds by poly(D,L-lactic acid) modification. *Acta Biomater.* **4**, 343–353. (doi:10.1016/j.actbio.2007.08.010)

Wu, C., Ramaswamy, Y., Gale, D., Yang, W., Xiao, K., Zhang, L., Yin, Y. & Zreiqat, H. 2008*c* Novel sphene coatings on Ti-6Al-4V for orthopedic implants using sol-gel method. *Acta Biomater.* **4**, 569–576. (doi:10.1016/j.actbio.2007.08.010)

Wu, C., Ramaswamy, Y., Chang, J., Woods, J., Chen, Y. & Zreiqat, H. 2008 The effect of Zn contents on phase composition, chemical stability and cellular bioactivity in Zn–Ca–Si system ceramics. *J. Biomed. Mater. Res. B Appl. Biomater* **87B**, 346–353. (doi:10.1002/jbm.b.31109)

Xue, W., Liu, X., Zheng, X. & Ding, C. 2004 Plasma-sprayed diopside coatings for biomedical applications. *Surf. Coat. Technol.* **185**, 340–345. (doi:10.1016/j.surfcoat.2003.12.018)

Xue, W., Liu, X., Zheng, X. & Ding, C. 2005 *In vivo* evaluation of plasma-sprayed wollastonite coating. *Biomaterials* **26**, 3455–3460. (doi:10.1016/j.biomaterials.2004.09.027)

Zheng, X., Huang, M. & Ding, C. 2000 Bonding strength of plasma-sprayed HAp/Ti composite coatings. *Biomaterials* **21**, 841–849. (doi:10.1016/S0142-9612(99)00255-0)

Zreiqat, H., Evans, P. & Howlett, C. R. 1999 Effect of surface chemical modification of bioceramic on phenotype of human bone-derived cells. *J. Biomed. Mater. Res.* **44**, 389–396. (doi:10.1002/(SICI)1097-4636(19990315)44:4<389::AID-JBM4>3.0.CO;2-O)

Zreiqat, H., Howlett, C. R., Zannettino, A., Evans, P., Schulze-Tanzil, G., Knabe, C. & Shakibaei, M. 2002 Mechanisms of magnesium-stimulated adhesion of osteoblastic cells to commonly used orthopaedic implants. *J. Biomed. Mater. Res.* **62**, 175–184. (doi:10.1002/jbm.10270)

Zreiqat, H., Valenzuela, S. M., Nissan, B. B., Roest, R., Knabe, C., Radlanski, R. J., Renz, H. & Evans, P. J. 2005 The effect of surface chemistry modification of titanium alloy on signalling pathways in human osteoblasts. *Biomaterials* **26**, 7579–7586. (doi:10.1016/j.biomaterials.2005.05.024)